Published in final edited form as:
Exp Cell Res. 2007 January 1; 313(1): 195–209.

Recruitment of phosphorylated small heat shock protein Hsp27 to nuclear speckles without stress

A. L. Bryantsev[1], **M. B. Chechenova**[1], and **E. A. Shelden**[1,2]

1 *School of Molecular Biosciences, Washington State University, Pullman, WA*

2 *Center for Reproductive Biology, Washington State University, Pullman, WA*

Abstract

During stress, the mammalian small heat shock protein Hsp27 enters cell nuclei. The present study examines the requirements for entry of Hsp27 into nuclei of normal rat kidney (NRK) renal epithelial cells, and for its interactions with specific nuclear structures. We find that phosphorylation of Hsp27 is necessary for the efficient entry into nuclei during heat shock but not sufficient for efficient nuclear entry under control conditions. We further report that Hsp27 is recruited to an RNAse sensitive fraction of SC35 positive nuclear speckles, but not other intranuclear structures, in response to heat shock. Intriguingly, Hsp27 phosphorylation, in the absence of stress, is sufficient for recruitment to speckles found in post-anaphase stage mitotic cells. Additionally, pseudophosphorylated Hsp27 fused to a nuclear localization peptide (NLS) is recruited to nuclear speckles in unstressed interphase cells, but wildtype and nonphosphorylatable Hsp27 NLS fusion proteins are not. The expression of NLS-Hsp27 mutants does not enhance colony forming abilities of cells subjected to severe heat shock, but does regulate nuclear speckle morphology. These data demonstrate that phosphorylation, but not stress, mediates Hsp27 recruitment to an RNAse soluble fraction of nuclear speckles and support a site-specific role for Hsp27 within the nucleus.

Keywords

Hsp25; Hsp27; epithelial; nucleus; mRNA; heat shock

INTRODUCTION

Hsp27 is a widely distributed member of the small heat shock protein (sHsp) family, having chaperone function in vitro [1], and providing tolerance to injury of cells in vivo (see [2] for review). Elevated expression and altered phosphorylation of Hsp27 characterize a number of disease states including cancer [3], and mutation of Hsp27 has been linked to the development of human neuropathology [4]. Despite consequent interest in cellular roles played by Hsp27, neither the mechanism nor function of Hsp27 are fully understood. Experimental evidence supports a variety of roles for Hsp27, including a general chaperone activity [1,5,6], interaction with actin cytoskeleton elements [7–10], interaction with pro- and anti- apoptotic signaling factors [11–13], and modulation of the oxidative balance of cells [14]. These activities can occur throughout the cell or are restricted to the cytoplasmic cell compartment. However, a

Address Correspondence to: Eric A. Shelden, Ph.D., Associate Professor, School of Molecular Biosciences, Washington State University, Pullman, WA 99164-4234, Email: eshelden@wsu.edu, Phone: 509-335-2368, Fax 509-335-1907

striking feature of Hsp27 is its stress-inducible entry into nuclei of some cells, accompanied by phosphorylation. Because Hsp27 promotes protein refolding, nuclear Hsp27 may interact with proteins in nuclei to promote refolding or target damaged proteins for degradation. In support of this view, Hsp27 in the nucleus of heat-shocked cells partially co-localizes with focal accumulations of damaged nuclear luciferase [9] and Hsp27 over-expression promotes resolubilization of nuclear protein in cells during recovery from heat shock [15].

In addition to acting as a general chaperone, it has been reported that Hsp27 may perform other functions in the cell and, especially, in the nucleus. For example, Hsp27 enhances recovery of protein synthesis [16] and mRNA splicing [17] in cells after heat stress. These beneficial effects of Hsp27 may be attributed, in part, to a chaperone function, leading to efficient reactivation of proteins required for mRNA processing during recovery from injury. Intriguingly, however, the related small heat shock protein alpha-B crystallin, like Hsp27, exhibits chaperone activity in vitro [1] and enters cell nuclei during stress [18], yet had no effect on mRNA processing activity in a previous study [17]. There exists, therefore, a disconnection between the general chaperone activity of mammalian small heat shock proteins and their effects within the nucleus. These findings indicate there may be specific substrates for Hsp27 within cell nuclei. Results of morphological studies support this hypothesis. Hsp27 is not uniformly distributed within the nuclear compartment of stressed cells, but rather, in most cells studied associates prominently with intranuclear granules [9,19–21]. The nuclear compartment contains numerous granular structures including nucleoli and concentrations of proteins involved in the processing or storage of mRNA and associated modifying proteins. These latter structures can be discriminated by analysis of their constituent proteins and include nuclear speckles, gems, Cajal bodies, promyelocytic leukemia nuclear (PML) bodies and others. In addition, nuclei of stressed cells recruit stress response elements including stress-inducible transcription factor HSF1 to structures known as stress granules that are distinct from nuclear bodies present in unstressed cells [22]. In recent studies, alpha-B crystallin was shown to associate in a phosphorylation dependent manner with a number of nuclear bodies involved in mRNA processing [23–25]. Intriguingly, this association occurred in the absence of stress in mitotic cells prior to reformation of the nuclear compartment. In addition, a small but detectable fraction of alpha-B crystallin was localized to nuclear bodies in unstressed interphase cells [24,25]. Together these previous results raise questions regarding mechanisms regulating Hsp27 within nuclei, its nuclear targets, and the role of stress in recruitment of Hsp27 to specific target sites.

The present study was conducted to specifically determine the manner in which the interaction of Hsp27 with nuclear structures is regulated, and the role of stress in this process. The entry of Hsp27 into the nucleus of cells has been previously shown to correlate strongly with Hsp27 phosphorylation [9,26,27]. However, biochemical isolates of nuclear Hsp27 contain nonphosphorylated Hsp27 [26], leaving the regulatory state of Hsp27 at specific sites within the nucleus unresolved. Here, we examined the distribution of endogenously expressed Hsp27 in nuclei of heat shocked normal rat kidney renal epithelial (NRK) cells and in mitotic cells, after manipulation of Hsp27 phosphorylation states. In addition, we examined the localization of exogenously expressed phosphorylation state mutants of human Hsp27 and their fusion proteins with nuclear localization (NLS) tags. Our results demonstrate that phosphorylation is necessary but not sufficient for efficient entry of Hsp27 into the nucleus. In contrast, we report that phosphorylation, but not stress itself, regulates association of Hsp27 to nuclear speckles. Finally, our results also differ from recent results obtained from study of the related small heat shock protein alpha-B crystallin [24,25]; Hsp27 was recruited exclusively to nuclear speckles in heat shocked cells and Hsp27 could be disassociated from nuclear speckles by RNAse treatment. Our data support the conclusion that Hsp27 plays regulatory roles in the nucleus that are distinct from activities performed by nuclear alpha-B-crystallin.

MATERIALS AND METHODS

Antibodies and reagents

Pan-specific anti-Hsp27 monoclonal 8A7 antibody was a gift from Dr. M. Welsh (University of Michigan). Species-specific polyclonal antibodies against rodent (SPA801) and human (SPA803) Hsp27 were purchased from StressGen Biotechnologies (Victoria, BC, Canada). The anti-SC35 antibody, DABCO, and RNAse A were purchased from Sigma (Sigma-Aldrich, St Louis, MO). Vanadyl riboside complex (Va) was obtained as a 200 mM stock solution from New England Biolabs (Ipswich, MA). DNAse I was ordered from Worthington Biochemical Corp. (Lakewood, NJ). All secondary antibodies were from Jackson ImmunoResearch Laboratories Inc. (West Grove, PA). Inhibitors were dissolved in DMSO. Anisomycin (Sigma) was used at a final concentration of 10 μg/ml. The p38 MAPK inhibitor SB202190 (Calbiochem) was used at a final concentration of 10 μM. Actinomycin D was used at a final concentration 2 μg/ml.

Plasmids

All Hsp27 expression vectors containing nuclear localization sequences were created from an initial plasmid (pcDNA3.1-h27SacII) containing the coding sequence for human Hsp27 with additional *Sac*II and *Eco*RV restriction sites placed at the 3′ end of the Hsp27 CDS. The plasmid was created by PCR amplification of a human Hsp27 ORF with forward 5′-CGGATCCATGACCGAGCGCCGCGT-3′ and reverse 5′-TTAGATATCCGCGGTCTCATCGGATTTTGCAGC-3′ primers and insertion of the PCR product into *Bam*HI-*Eco*RV sites of pcDNA3.1(+) (Invitrogen Corp., Carlsbad, CA). pcDNA3.1-h27SV40 containing the human Hsp27 ORF and the SV40 nuclear localization amino acid sequence KPKKKRKV at its 3′ end was created by annealing oligonucleotides 5′-GGCCAAGCCTAAGAAGAAGCGAAAGGTTGGC-3′ and 5′-GCCAACCTTTCGCTTCTTCTTAGGCTTGGCCGC-3′ and inserting the resulting double-stranded DNA fragment into the *Sac*II–*Eco*RV sites of pcDNA3.1-h27SacII. Similarly, a plasmid (pcDNA3.1-h27SV40mut) coding for human Hsp27 with a mutated SV40 NLS (KPTKKRKV) was created using oligonucleotides 5′-GGCCAAGCCTAAGACAAAGCGAAAGGTTGGC-3′ and 5′-GCCAACCTTTCGCTTTGTCTTAGGCTTGGCCGC-3. Plasmids for expression of NLS-tagged human Hsp27 mutants with replacement of serines 15, 78 and 82 with alanine (Hsp27-3A-NLS) and aspartic acid (Hsp27-3D-NLS) were created by excising a 1413 bp *Xcm*I-*Sma*I fragment from pcDNA3.1-h27SV40 and inserting this fragment into the *Xcm*I-*Sma*I sites of pcDNA3.1-h27(3A) and pcDNA3.1-h27(3D) (gift of Dr. R. Benndorf, University of Michigan).

A plasmid for expression of EGFP, NLS tagged luciferase (pnGL3-EGFP) was produced by PCR of the plasmid pGL3-basic (Promega Corp., Madison, WI), using forward and reverse primers 5′-AACTGCAGGCCACCATGGAAGAC-3′ and 5′-CGGGATCCACGGCGATCTTTC-3′, respectively. The resulting PCR product was inserted into the *Bam* HI and *Pst* I restriction sites of pEGFP-N1 (BD Bioscience Clontech, Mountain View, CA) to obtain pGL3-EGFP.

Finally, an NLS was added by digesting pGL3-EGFP and previously described pN-luc-EGFP [28] with *Kas* I and replacing the fragment containing the first 86 bp in the 5′ end of the luciferase gene in pGL3-EGFP with the corresponding NLS-containing fragment of pN-luc-EGFP. The fidelity of all constructed plasmids was verified by direct sequencing.

Plasmids coding for Sp100-YFP and SF2-EGFP were a gift from Dr. D. Spector (Cold Spring Harbor Laboratory, NY). The plasmid coding for mouse coilin fused to EGFP was provided

by Dr. G. Matera (Case Western Reserve University, OH) and the proliferating cell nuclear antigen (PCNA)-GFP expressing plasmid was provided by Dr. R. Kanaar (Erasmus Medical Center, Rotterdam, The Netherlands).

Cell culture and transfection

Normal rat kidney cell line NRK-52E and NIH3T3 murine fibroblasts (ATCC) were used up to 15th passage. NRK cells were grown in DMEM supplemented with 10% fetal bovine serum (Invitrogen, Carslbad, CA). NIH3T3 cells were grown in DMEM supplemented with 10% calf serum (Invitrogen). Cells were incubated at 37°C in an atmosphere of 5% CO_2 and 95% air and subcultured twice a week. For experimental use, cells were plated into 24-well plates at 5–6×10^4 cell/well or 6-well plates at 2×10^5 cell/well. Cell were transfected 24 hours after plating using Lipofectamine Plus reagents (Gibco BRL, Invitrogen). NRK cells were incubated over a 3 hour period with 0.3 μg plasmid DNA, 3 μl Plus reagent and 1 μl Lipofectamine in 300 μL DMEM. NIH3T3 fibroblasts were incubated over a 5 hour period using 0.5 μg plasmid DNA, 5 μl Plus, and 2 μl Lipofectamine. At the end of incubation, transfection media were replaced with growth medium or cells were subcultured into wells containing 12-mm diameter circular coverslips. Experimental studies were conducted 18–24 hours post transfection except as indicated.

Cell fractionation

Cell fractionation was carried out essentially as described previously [29,30] in the presence of protease (Roche Diagnostics Corp., Indianapolis, IN) and phosphatase (Sigma) inhibitor cocktails, used at the manufacturers recommended concentrations. Briefly, for immunofluorescence imaging studies of Hsp27 localization, cells were cultured on glass coverslips, then washed once with phosphate buffered saline (PBS) and lysed on ice for 5 minutes in CSK buffer (10 mM PIPES (pH 6.8), 100 mM NaCl, 300 mM sucrose, 3 mM $MgCl_2$, 1 mM EGTA, 0.5% Triton X-100, 4 mM vanadyl riboside complex (Va, New England Biolabs). To analyze effects of DNAse and RNAse treatment on retention of Hsp27 by detergent lysed cells (Figures 3 and 6), cells were also rinsed after lysis three times in Digestion Buffer (DB; 10 mM PIPES (pH6.8), 50 mM NaCl, 300 mM sucrose, 3 mM $MgCl_2$, 1 mM EGTA, 0.5% Triton X-100), and then treated at room temperature with 50 μg/ml RNAse A in DB either with or without Va (15 min) or with 150 μg/ml DNAse I in DB (20 min) prior to fixation. Cells were subsequently fixed for 10 minutes by adding 37% formaldehyde directly to the coverslips to a final concentration of 3.7% and processed for fluorescence detection of Hsp27 and other proteins. Alternatively, for biochemical studies, cells were grown in 6-well plates, extracted as described above and proteins extracted in each step precipitated from buffers with 5% TCA followed by centrifugation for 5 min at 20,000 × g at 4°C. Pellets were washed three times in ice-cold acetone and resolubilized in equal volumes (75 μl) of 9M urea, 1% Nonidet P40, 4% beta-mercaptoethanol, and anti-phosphatase inhibitors. Equal volumes of samples were then loaded onto gels for analysis of the relative presence of Hsp27 in different samples as well as its isoelectric focusing points.

Isoelectric focusing, electrophoresis, and Western blotting

Isoelectric focusing (IEF) gel electrophoresis was performed as described elsewhere [31]. 10–15 μl samples were prepared in IEF buffer (9M urea, 1% Nonidet P40, 4% beta-mercaptoethanol, anti-phosphatase inhibitor cocktail) and loaded on IEF slab gels containing 7.5% acrylamide, 9M urea, 4% ampholyte mixture (pH range 5–7, Sigma). Isoelectric focusing was performed at 450 V, 2 W, and 2,000 V/hour using a Mini IEF Cell (BioRad). SDS polyacrylamide gel electrophoresis (SDS PAGE) was performed in 12% acrylamide gels. For Western blotting, proteins were transferred onto nitrocellulose membrane at 300 mA for 2 hours. Membranes were probed with either the monoclonal 8A7 or polyclonal anti-human

Hsp27 SPA803 and appropriate horseradish peroxidase-labeled secondary antibodies. Chemiluminescent detection was carried out by means of AutoBioChemi System (UVP Inc., Upland, CA). Quantitative analysis of Western blots was conducted using dedicated image analysis software (LabWorks, UVP Inc.).

Immunofluorescence

Cells were washed in PBS, fixed in 3.7% formaldehyde for 10 minutes, permeabilized in 1% Triton X-100 for 15 minutes, and incubated with primary antibodies either overnight at 4°C or 1–2 hours at ambient temperature. Transfected human Hsp27 and all its variants were detected with a polyclonal human Hsp27-specific antibody (SPA803). Rodent Hsp27 was detected with rabbit serum SPA801. For double labeling studies, rabbit and mouse primary antibodies were applied together. Goat polyclonal antibodies labeled with FITC or Cy3 were used as secondary antibodies. Immunostained cells were mounted on glass microscope slides using polyvinyl alcohol mounting media containing 100 mg/ml DABCO as anti-fading reagent. Most slides were imaged with a fluorescence microscope Axiovert 200M, using AxioVision Software (both from Carl Zeiss Inc., Thornwood, NY). Immunolocalization studies shown below in Figures 2 and 5C were conducted using a Zeiss LSM510 META confocal microscope operated in its Multiscanning mode. Figures were assembled using Adobe Photoshop and Adobe Illustrator software (both from Adobe Systems Inc., San Jose, CA).

Image Analysis

For each protocol, a sufficient number of randomly selected fields of cells were imaged to obtain a samples size of about 50 nuclei for each experimental procedure. To analyze the efficiency of nuclear entry (Figure 1), images of transfected cells were first assigned a random alphanumeric code. The total number of transfected cells and the number of cells with nuclear Hsp27 in each image were then counted by a blinded investigator. To assess the efficiency that expressed proteins associated with nuclear speckles (Figure 7), images of transfected cells were again randomized prior to analysis. Images were imported into ImageJ, a freeware image analysis package maintained by the National Institute of Health. Nuclei of transfected cells were outlined with a region of interest (ROI) using a Wacom digitizing tablet and pen, and the total fluorescence intensity within this ROI was calculated by the ImageJ program. Nuclear speckles were then counted and set to an intensity value of zero using an eraser tool. Where possible, fluorescence within nucleoli was excluded from this procedure and therefore contributed to the measured fluorescence intensity of the background. Fluorescent nucleoli were seen in cells expressing with NLS-Luc-GFP (Figure 7B, Luc-NLS), but not in cell expressing any Hsp27 protein. Each nucleus was again selected with a ROI and the total non-speckle fluorescence intensity measured. The value obtained for non-speckle fluorescence was subtracted from the initial (total fluorescence) value to derive the fluorescence intensity for all nuclear speckles in each cell. Because the fluorescence intensity of expressed Hsp27 at nuclear speckles must be determined in part by the overall expression level, the ratio of speckle versus non-speckle fluorescence was calculated. For quantitative analysis of nuclear speckle morphology in cells (Figure 9 and Table 1), images of 35 to 50 nuclei for each protocol were obtained of cells triple labeled for expressed Hsp27, DNA and SC35. Images of cell nuclei containing detectable exogenously expressed Hsp27 were selected and saved, followed by selection of an equal number of neighboring non-expressing cell nuclei of similar size. To avoid bias in selecting control nuclei, the second selection was made while viewing the DNA staining pattern, not the SC35 staining pattern. Images of nuclei were randomized and the number of SC35 positive nuclear speckles counted by a blinded investigator. For morphometric studies, images of cells were imported into ImageJ and a digital brightness threshold was applied to each image. The threshold was varied to select all nuclear speckles but only a small number of pixels in the diffuse background. In a preliminary analysis, we determined that all structures counted previously as nuclear speckles were larger than 20 pixels in area. A particle

analysis function available in the ImageJ program was applied to thresholded images, and the area and fluorescence intensity (FI) of nuclear speckles was measured using functions available in the ImageJ program. The volume of speckles was calculated from the measured area of each speckle, using the assumption that the image of a speckle is a 2-dimensional projection of a spherical object. Statistical comparison of data sets were performed with Microsoft Excel using a Student's two-sample T-test. Data sets were compared assuming unequal variance, with a hypothesized mean difference of zero (alpha of .05).

Cell survival assay

Assays of cell survival were conducted using a colony forming assay [32], with minor modifications. Briefly, NIH3T3 fibroblasts were transfected as described above using 0.5 μg/well of plasmid DNA. 24 hours after transfection cells were heated in an Isotemp 2150 water bath (Fisher Scientific, Pittsburgh, PA) at 44°C for 2.5 hours. Immediately afterwards, cells were trypsinized and plated into 100-mm culture dishes. After 7–10 days of culture, cells were fixed and stained with 0.5% Crystal Violet (in 50% methanol) and colonies containing more than 50 cells counted. To normalize survival rates among independent experiments, the total number of colonies in each experiment was summed and the ratio of colonies produced by each transfection in a given experiment was calculated. The average and standard deviation of these values were calculated for three independent experiments. Alternative experiments were conducted by transfecting cells with different amounts of Hsp27 coding plasmid. The total plasmid DNA concentration in these transfection experiments was kept constant by the addition of empty pcDNA3.1 vector. The stress treatment and colony formation assay was conducted as described above.

RESULTS

Hsp27 phosphorylation mediates entry into the nucleus of heat shocked NRK cells

Endogenous rat Hsp25 was found within the cytoplasm of normal rat kidney epithelial (NRK) cells under control conditions, as expected (Fig 1A, *CNTR*). In contrast, heat shock (43°C for 30 minutes) induced translocation of Hsp25 into the nucleus, as well as some association with fibrous cytoskeletal elements. The pattern of Hsp25 immunostaining within the nucleus of heat shocked NRK cells was characterized by both diffuse staining and prominent nuclear granules (Fig 1A, *HS*). Phosophorylation of Hsp25 was next examined in unstressed and heat shocked NRK cells using isoelectric focusing and immunoblotting. Unstressed NRK cells contained two isoforms of Hsp25 (Fig 1B, lane 1). Heat shock of NRK cells (Fig 1B, lane 2) was coincident with a reduced presence of the most basic isoform (*a*) and enrichment of more acidic isoforms (*b*,*c*), consistent with a reduction in nonphosphorylated protein and an increase in singly and doubly phosphorylated Hsp25.

Some nonphosphorylated Hsp25 remained in heat shocked NRK cells (Fig 1B, lane 2) as well as preparation of nuclear proteins in other studies [26]. To more specifically assess the role of phosphorylation in mediating entry of Hsp27 into the nucleus of NRK cells, distribution patterns of exogenously expressed wild-type and phosphoserine mutants of human Hsp27 were examined in cells under control conditions and after heat shock. These exogenously expressed proteins were specifically detected in NRK cells using antibodies recognizing only human Hsp27 (see Figure 4 and data not shown). Under control conditions, all of the exogenously expressed human Hsp27 protein variants were present primarily in the cytoplasm. A small proportion of transfected NRK cells also showed nuclear localization of expressed Hsp27 under control conditions (black bars, Fig 1C, -HS). The proportion of cells showing nuclear localization of exogenous protein was independent of the type of mutation present in the expressed protein. Heat shock induced the further appearance of wild-type human Hsp27 (WT) and a mutant Hsp27 protein mimicking constitutive phosphorylation (3D) in the nucleus (black

bars, Fig 1C, +HS). In contrast, the non-phosphorylatable Hsp27 mutant protein (3A) showed little increase in its presence in nuclei after heat shock. Similar results were obtained in NIH3T3 fibroblasts (not shown). Therefore, in NRK cells, Hsp27 phosphorylation does not appear sufficient for efficient entry into the nucleus under control conditions, but is necessary for efficient translocation into the nucleus during heat shock.

Hsp27 is recruited to nuclear speckles in heat shocked cells

We conducted co-localization studies of endogenous rat Hsp25 and specific nuclear domains in heat stressed NRK cells using confocal fluorescence microscopy (Fig 2). Because some antibodies may cross-react nonspecifically with nuclear antigens [33], markers for nuclear structures were provided by transient transfection of plasmids coding for the expressing of fluorescent fusion protein of specific nuclear proteins. Endogenous rat Hsp25 was recruited to nuclear granules in heat shocked NRK cells that also contained EGFP-SF2, a marker for nuclear speckles/interchromatin granules. Possible association of Hsp25 with PML domains, Cajal bodies and sites of DNA replication was also examined in heat shocked NRK cells expressing GFP/YFP-tagged Sp100, coilin or PCNA, respectively. However, Hsp25 did not detectably co-localize with any of these later probes after heat shock (Fig 2), although coilin containing Cajal bodies were often observed in a close proximity to the Hsp27 granules (Fig 2, inset). Note that Hsp25 was variably present as diffuse staining and granular bodies in the cytoplasm of all heat shocked NRK cells (Fig 2, Hsp25), but no fluorescent signal from fluorescent fusion proteins was detected in the cytoplasm (Fig 2, GFP/YFP). Therefore, the fluorescence signal from fluorescent fusion proteins could not have resulted from non-specific immunostaining or crossover of signal between fluorescent channels. Although co-localization studies were not conducted with probes specific for nucleoli, these largest of nuclear bodies are easily recognized by their exclusion of other probes in some images (see SF2 and PCNA images in Figure 2). It is evident that nucleoli did not recruit Hsp25 in these studies. Therefore, endogenous rat Hsp25 is recruited exclusively to nuclear speckles in heat shocked NRK cells and not to other structures examined in this study.

Phosphorylated Hsp27 is recruited to an RNAse soluble fraction of nuclear speckles

We next conducted studies to characterize the compartment recruiting endogenous Hsp25 in heat stressed NRK cells. Nuclear speckles were identified in these studies by counterstaining cells with antibodies against the splicing factor SC35. The top three panels in Figure 3 show the distribution of Hsp25, SC35 and DNA in intact cells after heat shock (Fig 3A, unlabeled). Detergent lysis of cells alone did not release Hsp25 from nuclear speckles or lead to detectable reduction in diffuse nuclear staining (Fig 3A, *Triton*). However, detergent lysis followed by treatment of cells with RNAse A (50 μg/ml, 30 minutes) abolished the presence of Hsp25 in nuclear speckles (Fig 3A, *RNAse*). There was also some reduction in diffuse nuclear staining after RNAse treatment. In contrast, DNAse (Fig 3A, *DNAse*) did not remove Hsp25 from nuclear speckles or noticeably alter diffuse staining, but did abolish staining of cells with DNA specific probe. RNAse treatment in combination with an RNAse inhibitor (not shown) also failed to remove Hsp25 from nuclear speckles. We conclude that RNA but not DNA is an element of structures recruiting endogenous rat Hsp25 to nuclear speckles, as well as a portion of diffuse nuclear staining.

The phosphorylation state of extracted Hsp25 was also directly examined (Fig 3B). Total Hsp25 in control cells was mostly non-phosphorylated (*a*, Fig 3B, lane 1). In contrast, all preparations from heat-shocked cells contained primarily phosphorylated Hsp25 (*b*,*c* Fig 3B, lanes 2–4,6). No fraction was enriched in non-phosphorylated Hsp25, even though a small but detectable amount of non-phosphorylated Hsp25 is clearly present in total cell lysates of heat shocked cells (Fig 3B, lane 2). DNase treatment did not detectably remove Hsp25 from lysed cell (Fig 3B, lane 5), and incubation of cells with RNAse in combination with RNAse inhibitors greatly

limited the amount of extracted Hsp25 (Fig 3B, lane 6), consistent with results shown in Figure 3A. These results show that the RNAse soluble fraction of the nucleus does not preferentially recruit non-phosphorylated Hsp25, and may specifically recruit the phosphorylated form. Studies below directly test this hypothesis.

Mitotic interchromatin granules selectively recruit phosphorylated Hsp27 in the absence of stress

To establish the role of stress in recruiting Hsp27 to nuclear speckles, we first examined the distributions of endogenous Hsp25 and the nuclear speckle protein SC35 in mitotic NRK cells. During late stages of mitosis, nuclear speckles organize in the cytoplasm, forming structures called mitotic interchromatin granules (MIGs) [34] that are accessible to proteins not normally found within the interphase nucleus. Untreated telophase NRK cells had only diffusely distributed Hsp25 (Fig 4A, CNTR, Hsp25), but displayed prominent SC35 positive MIGs in the cytoplasm (Fig 4A, - CNTR, SC35). Brief exposure of cells to anisomycin, an activator of p38-MAPK dependent signaling pathways, results in enhanced phosphorylation of endogenous Hsp25 ([35] and Fig 4B, *lane 2*). Anisomycin treatment also induced colocalization of endogenous Hsp25 with SC35 positive MIGs (Fig 4A, +ANISO). To test if Hsp25 was recruited to MIGs in telophase cells because of possible unrelated effects of anisomycin, we pre-incubated cells with the p38 MAPK inhibitor SB202190. SB202190 pre-treatment blocked anisomycin induced accumulation of Hsp25 in MIGs (Fig 4A +A+SB) as well as the phosphorylation of Hsp25 phosphorylation by anisomycin (Fig 4B, *lane 3*).

We next expressed human Hsp27 mutants mimicking constitutive phosphorylation (3D) or abolishing phosphorylation (3A) in NRK cells and examined their distributions in telophase NRK cells without other manipulations (Fig 4). Note that antibodies specific for human Hsp27 detect the exogenous human Hsp27 protein in transfected cells, but not neighboring untransfected cells (asterisks) in these images (Fig 4C, SC35). Therefore, the antibodies used for these studies detect only human Hsp27 and do endogenous rat Hsp25. The human Hsp27 mutant lacking phosphorylatable serines (3A) did not associate with MIGs under control conditions (not shown) or in cells treated with anisomycin (Fig 4C, +ANISO, *3A*). In contrast, the Hsp27 mutant mimicking the phosphorylated state constitutively associated with MIGs in untreated cells (Fig 4C, CNTR, *3D*). Together, the results obtained from the analysis of both endogenous rat Hsp25 (Fig 4A,B) and human Hsp27 mutants (Fig 4C) demonstrate that SC35 positive granules in mitotic cells specifically recruit phosphorylated Hsp27 in the absence of heat shock.

Nuclear speckles selectively recruit phosphorylated Hsp27

Under control conditions, interphase NRK cells exclude both endogenous rat Hsp25 and human Hsp27 phosphorylation state mimicking mutants from the nucleus (Figs 1A, C). To study association of Hsp27 with nuclear speckles in the intact interphase nucleus, we created expression vectors for novel NLS-tagged versions of wild-type and mutant human Hsp27 (Fig 5A) and assessed distributions of expressed proteins in nuclei of unstressed NRK cells (Fig 5B). Most transfected cells displayed normal nuclear architecture, characterized by diffuse staining of DNA in interphase cells with DNA specific fluorescent dyes (Fig 5B, *DNA*). A variable minority of cells displayed unusually condensed DNA. Quantitation of the proportion of such cells as a total of transfected cells revealed that the number of these unusual cells was invariant and not dependent on the phosphorylation state of expressed Hsp27 (not shown). In all other cells, Hsp27-WT-NLS and Hsp27-3A-NLS proteins were excluded from nucleoli but were otherwise homogeneously distributed within the nucleus of interphase cells (Fig 5B, *WT-NLS, 3A-NLS*). In contrast, HSP27-3D-NLS protein show a granular pattern within interphase nuclei of unstressed NRK cells (Fig 5B, *3D-NLS*) that closely resembles that of endogenous rat Hsp25 in nuclei of NRK cells after heat shock (Fig 1A).

Stress dramatically alters regulation of cellular proteins within the nucleus and other cell compartments. We therefore asked if the specific pattern of recruitment shown by endogenous Hsp25 in heat shocked NRK cells could be replicated in unstressed interphase cells by phosphorylation-state mimicking NLS-tagged Hsp27. Indeed, Hsp27-3D-NLS protein co-localized with SC35 positive nuclear speckles (yellow/orange, Fig 5C, Overlay) in the absence of heat shock but not with PML domains, Cajal bodies, or sites of DNA replication (Fig 5C). We also assessed the solubility of NLS-tagged Hsp27-3D mutant proteins associated with nuclear speckles, using biochemical approaches. First, Hsp27-3D-NLS associated with SC35 positive nuclear speckles (Fig 6B, *Triton*), like the endogenous, speckle associated Hsp25 found in heat shocked cells (Fig 3A). Also like endogenous phosphorylated Hsp25, treatment of detergent lysed cells with RNAse removed Hsp27-3D-NLS protein from nuclear speckles (Fig 6B, RNAse −Va), but an identical incubation in the presence of both RNAse and RNAse inhibitor (Fig 6B, RNAse +Va) did not. Diffuse nuclear staining for endogenous Hsp25 was retained in heat shocked cells under our experimental conditions (Figure 3) but diffuse staining for the Hsp27-3D-NLS was removed by detergent alone in control cells (Figure 6, *TRITON).* Therefore there may be targets present in heat shocked cells that the Hsp27-3D-NLS mutant did not interact with under control conditions. However, our data do support the conclusion that Hsp27-3D-NLS is recruited to nuclear speckles in unstressed interphase NRK cells using a mechanism that in our studies is indistinguishable from that recruiting endogenous phosphorylated Hsp25 to nuclear speckles during heat shock.

We also quantified the extent of nuclear speckle localization for NLS-tagged Hsp27 protein expressed in NRK cells after heat shock. An NLS-tagged GFP-luciferase fusion proteins, shown previously to associate with nuclear speckles and nucleoli of heat shocked H9C2 myoblasts [9] was examined here as a non-specific control (Figure 7A). The average fluorescence intensity of NLS-Luc-GFP protein associated with nuclear speckles was about 15% as great as that measured for diffuse background nuclear fluorescence in the same cell. Hsp27-WT-NLS and Hsp27-3D-NLS fusion proteins both associated with nuclear speckles to a statistically greater extent, with the Hsp27-3D-NLS fusion protein showing the greatest tendency to associate with nuclear speckles. In contrast, nuclear speckles recruited the non-phosphorylatable Hsp27-3A-NLS mutant to a significantly lower extent than that of even the control NLS-Luc-GFP protein, with many cells showing no localization to nuclear speckles (not shown). Figure 7B shows the fluorescence staining pattern of cells having the median calculated ratio (+.02) of speckle-specific and diffuse fluorescence in each group. Notably, fluorescence from nuclear speckles in cells expressing Hsp27-WT-NLS and especially Hsp27-3D-NLS is much greater than that seen in cells expressing Hsp27-3A-NLS and NLS-Luc-GFP proteins.

Nuclear tagged Hsp27 alters regulation of nuclear speckles, but not colony formation after heat shock

Studies above reveal that stress is not necessary for interaction of Hsp27 with nuclear structure and that a nuclear targeted Hsp27 mutant mimicking constitutive phosphorylation displays all tested features of endogenous Hsp27 within the nucleus of heat shocked cells. We therefore examined functional consequences of the expression of NLS-tagged Hsp27 proteins. To avoid potential complications of the expression of endogenous protein, these studies were conducted using murine NIH3T3 fibroblasts that do not detectably express endogenous Hsp25 under control conditions ([36] and not shown). Immunolocalization studies confirmed that NLS-tagged proteins entered nuclei of NIH3T3 cells (not shown). As shown in Figure 8A, transfection of NIH3T3 fibroblasts with expression vectors coding for wild type Hsp27, but not Hsp27 WT-NLS or the unrelated EGFP, promoted colony formation by cells after severe heat shock in a dose-dependent manner. Figure 8B compares effects produced by transfection with 0.5μg of plasmid expression vector for different proteins. Expression of a wild-type Hsp27

protein containing a nonfunctional NLS tag (Hsp27-NLSmut) was, on average, almost as effective in promoting colony formation after heat shock as wild type Hsp27 (Fig 8B). The difference in number of colonies formed by heat shocked cell cultures transfected with wild-type Hsp27 and Hsp27-NLSmut expression vectors were not statistically different ($p>0.1$). In contrast, cells expressing NLS tagged Hsp27 wild-type and phosphorylation mutants showed no greater colony forming abilities than cells transfected with an empty vector or an EGFP expression vector (Fig 8B). Transfection with vectors for expression of NLS-tagged Hsp27 mutants also did not reduce the number of colonies formed by transfected cells, relative to cells transfected with empty vector or an unrelated EGFP expression vector (Fig 8B).

The inhibition of mRNA synthesis using actinomycin D rapidly alters the number and size of nuclear speckles, revealing the dynamic nature of these structures [37]. Here, we examined the number and size of SC35 positive nuclear speckles in cells expressing either Hsp27-3A-NLS or Hsp27-3D-NLS alone and after varying times of treatment with actinomycin D. The presence of Hsp27 in nuclei was confirmed by counterstaining cells with antibodies recognizing human Hsp27 (not shown), and neighboring non-expressing cells were analyzed in each experiment to provide internal controls. Under control conditions, cells expressing Hsp27-3A-NLS did not appear different from nontransfected controls, but cells expressing Hsp27-3D-NLS appeared to have fewer and larger nuclear speckles (Fig 9A, *0′*). Quantitative analysis of the number of nuclear speckles in individual nuclei confirmed that these apparent differences were statistically significant (Fig 9B). Actinomycin D treatment resulted in reorganization of nuclear speckles into larger and fewer granules in a time-dependent manner (Fig 9, unlabeled top panels). Cells expressing Hsp27-3D -NLS protein, but not cells expressing Hsp27-3A-NLS protein, displayed a persistent, statistically significant, reduction in the number of nuclear speckles compared to non-expressing internal controls (Fig 9A, B). On average, cells expressing Hsp27-3A-NLS had about one third fewer granules than non-expressing cells in the same field (Fig 9B, Table 1), but greater differences were measured in some individual experiments (not shown). The size and fluorescence intensities of nuclear granules were also measured and compared in nontransfected cells and neighboring cells expressing Hsp27-3D-NLS protein after 120 minutes of actinomycin D treatment (Table 1). Results of this analysis confirms that although the number of nuclear speckles in Hsp27-3D-NLS expressing cells decreased, relative to nontransfected cells, the size and immunofluorescence intensities of nuclear speckles increased. Thus, it appears that the loss of nuclear speckle number in Hsp27-3D-NLS expressing cells, relative to control cells, is a consequence of the reorganization of nuclear speckles into larger structures.

DISCUSSION

Nuclear accumulation of Hsp27 is a common effect of cell stress and is seen in response to heat shock [9], ischemia/re-oxygenation [20], UV irradiation [27], toxin exposure and other stresses [19]. The present study was designed to establish mechanisms regulating entry and distribution of Hsp27 within the nuclear compartment. Our results add to existing data illustrating cell-type specific entry of Hsp27 into the nuclear compartment of cells. For example, Geum et al reported constitutive entry of Hsp25 mutants mimicking phosphorylation into nuclei of unstressed hippocampal neuron progenitor cells [26]. Constitutive entry of *Drosophila* Hsp27 into nuclei of developing oocytes has also been reported [38], and a related 26 kDa small heat shock protein expressed in *Artemia* also enters nuclei of cells in a developmentally regulated manner [39]. In contrast, Adhikari et al noted that both Hsp25 and related alpha-B crystallin were excluded from nuclei of mature myocytes, but not immature myoblasts, under all tested conditions, including heat shock [21]. Here, Hsp27 displayed an intermediate ability to enter nuclei of NRK renal epithelial cells; all tested proteins were excluded from the majority of unstressed cells, and the phosphorylation state of tested proteins had no effect on the small number of unstressed cells with nuclear Hsp27. These results suggest

some aspect of transfection, likely transient high-level expression of exogenous proteins or the reagents used for transfection in the present study, can non-specifically promote entry or retention of Hsp27 in nuclei of some NRK cells. Alternatively, dividing unstressed NRK cells may contain Hsp27 in nuclei at some, but not all stages of the cell cycle. Consistent with previous studies, heat stress greatly increases the number of NRK cells showing nuclear localization of the phosphorylation-competent Hsp25, as well as the phosphorylation state mimicking human Hsp27-3D mutant, while the Hsp27-3A mutant protein lacking serines at positions 15, 78 and 82, was largely excluded from the nucleus, even in heat shocked cells. Our studies do not address the issue of whether phosphorylation at all of these sites is required. However, the previous and current data are sufficient to demonstrate that entry of human Hsp27 into the nucleus requires phosphorylation at serines 15, 78 and 82 or some combination of these sites. Because the pseudophosphorylated Hsp27-3D mutant was largely excluded from nuclei of cells under control conditions, other factors may also play a determining role in this process. Such factors could include further modifications of Hsp27, such as phosphorylation at threonine 143 [40] and S-thiolation of cysteine 137 [41], as well as the functional size of nuclear pores, shown previously to be both variable and cell-type specific [42].

A cell-type specific presence of Hsp27 in the nucleus is suggestive of a regulatory role for Hsp27 in the nuclear compartment, in addition to more universal protective roles occurring in the cell cytoplasm. This view of Hsp27 function is indirectly supported by a disconnection between the abilities of Hsp27 and related small heat shock proteins to promote cell survival during injury and their presence in the cell nuclei. For example, in the present study, forced insertion of Hsp27 into the nucleus of NIH3T3 cells by addition of NLS tags did not promote colony formation of cells subjected to a severe heat shock. It remain possible that NLS tags could have interfered with some aspects of Hsp27 function in the nucleus. However, it is notable that NLS tagged proteins display distributions within the nucleus consistent with that expected from study of endogenous proteins, and the addition of a non-functional NLS to Hsp27 did not significantly reduce the ability of tagged Hsp27 to promote colony formation by cells after heat shock, relative to an untagged positive control. Similarly, studies by Borrelli and co-workers showed that an EGFP-Hsp27 fusion protein too large to detectably enter the nucleus of cells promoted survival of heat shocked cells to the same degree as wild-type Hsp27 [43]. Further support for a role of nuclear Hsp27 independent of the promotion of cell survival has come from comparative studies examining RNA processing in cells transfected with expression vectors for either Hsp27 or the related alpha-B crystallin [17]. Both of these small heat shock proteins display chaperone ability in vitro [1] and promote thermotolerance of heat-shocked cells [7,44]. However, in recent studies, Hsp27 enhanced the restoration of mRNA splicing activity in cells during the recovery from heat shock, while alpha-B crystallin had no effect in this assay system [17]. Thus, while the role of Hsp27 in the nucleus of stressed cells must be relevant to some aspect of the cellular stress response, the relationship between nuclear Hsp27 and the ability to withstand greater than normal levels of stress before cell death occurs appears to be increasingly distant. The ability of an individual cell to survive during a given stress event may therefore involve mechanisms related but distinct from those involved in restoring normal functionality once the stress event has passed, although both processes are clearly of importance to an intact tissue or organism. Data obtained in the present and previous studies suggest that cytosolic Hsp27 plays a role in the former process while a role for nuclear Hsp27 in the latter process is supported.

What is the function of Hsp27 in nuclear speckles? Hsp27 promotes refolding of denatured proteins in vitro [1] and has been associated with concentrations of unfolded nuclear reporter proteins in vivo in heat shocked cells [9]. Overexpression of Hsp27 enhances resolubilization of heat-denatured nuclear proteins in cells [15]. Although early studies indicated that non-phosphorylated Hsp27 was primarily effective in generating thermotolerance and chaperone activities [45,46], in some studies Hsp27 mutants mimicking the phosphorylated state show

effective chaperone activity for specific substrates such as actin [47]. Unpublished data also indicate that the Hsp27-3D mutant but not the Hsp27-3A mutant provides the best refolding rates for a heat inactivated firefly luciferase in vivo (Bryantsev et al, in press). These and other observations demonstrate that Hsp27, even in its phosphorylated state, may act as a molecular chaperone within the cell nucleus. However, whether it does so at particular sites within the nucleus remains unclear. For example, a chaperone model of Hsp27 function is difficult to reconcile with data obtained in the present study showing phosphorylation-dependent interaction of both endogenous Hsp25 and exogenous human Hsp27 with nuclear speckles without stress. Instead, our data suggest that Hsp27 associated with nuclear speckles could support specific activities of nuclear speckles during stress or recovery from stress.

The inhibition of gene expression and mRNA processing, and restoration of these activities during recovery, are essential and conserved cell responses to sublethal injury [48]. Functional changes to proteins found in nuclear speckles are responsible for these events and could be targets for Hsp27 within nuclear speckles. In support of this view, overexpression of Hsp27, but not alpha-B crystallin, was recently shown to promote restoration of normal mRNA splicing activity as well as the inactivation by phosphorylation of SRp38, a negative regulator of splicing activity [17]. However, it is still unclear whether Hsp27 present in nuclear speckles is directly involved in this regulation. Nuclear speckles are not generally considered to be directly involved in splicing activity, but may serve as splicing factor reservoirs or processing sites [37]. Additionally, SRp38 did not associate with SC35 positive nuclear speckles in cells under control conditions or after heat shock [49] yet Hsp27 clearly does. We note that diffuse, detergent soluble Hsp27 was detected in our studies, and could be involved in directly regulating SRp38. In addition, Hsp27 associated with nuclear speckles could play an indirect role in regulating mRNA processing by accelerating the release of splicing factors or other regulatory elements from nuclear speckles during the recovery from stress. However, these potential functions are not strongly supported by current data. An alternative possibility is that Hsp27 plays a direct role in regulating the function of nuclear speckles during the cellular response to injury. Recent work by Spector and colleagues has demonstrated that nuclear speckles are storage sites for mRNAs coding for proteins required for efficient cell recovery after stress [50]. The mechanism(s) regulating the storage and release of these unique mRNA molecules is presently unknown. The presence of Hsp27 within nuclear speckles may participate in the activation of this response. Ultimately, identification of the targets for Hsp27 in unstressed cells will be necessary to resolve these issues.

Finally, our studies provide some new insight into the unique functions of Hsp27 and alpha-B crystallin. These two proteins share extensive sequence homology and are often expressed in a single cell type. As noted above, both proteins display chaperone activity in vitro, can be phosphorylated at multiple serines, and provide protection against thermal injury when overexpressed in cultured cells. In addition, both proteins enter nuclei of some cell types during injury and interact with nuclear speckles. Despite their similarities, these proteins display subtly distinct roles and patterns of regulation in comparative in vivo studies. For example, in the cytoplasm of striated muscle cells, both Hsp27 and alpha-B crystallin can associate with myofibrils during injury, but the extent and dynamics of this interaction differ [33]. Cytoplasmic Hsp27 is also thought to interact primarily with actin microfilaments [51], while cytoplasmic alpha-B crystallin appears most frequently to interact with intermediate filament proteins (see [52] for review). A similar distinction appears in the nuclear function of these proteins. Both Hsp27 and alpha-B crystallin have been shown to interact with nuclear granules in nuclei of injured cells. Additionally, alpha-B crystallin interacts with nuclear speckles in the absence of stress, and in a phosphorylation dependent manner [21,25,53]. Here, we have shown a highly similar pattern of interactions for Hsp27. However, alpha-B crystallin associates with numerous mRNA processing structures in cell nuclei, including nuclear speckles, gems, and Cajal bodies [25]. In contrast, Hsp27 was seen in the present study to associate exclusively

with nuclear speckles. Additionally, nuclear speckle-associated alpha-B crystallin was resistant to extraction by both DNAse and RNAse in previous studies [25], while in contrast Hsp27 in the present study was readily extracted from nuclear speckles by RNAse yet was unaffected by DNAse treatment. Results of the present study suggest that Hsp27 and alpha-B crystallin perform distinct function in the nucleus in part through their recruitment to unique targets that can be distinguished based on morphological and biochemical criteria.

Acknowledgements

We thank Dr. David Spector (Cold Spring Harbor Laboratories, NY), Dr. Gregory Matera (Case Western Reserve University, OH), and Dr. Ronald Kanaar (Erasmus Medical Center, Rotterdam, The Netherlands) for providing expression vectors for fluorescent fusion proteins used in this study. We also thank Drs. Benndorf and Welsh (University of Michigan) for critical reading of a draft of this manuscript. This work was supported by a grant from the National Institute of Environmental Health Sciences (ES1196) to EAS.

References

1. Jakob U, Gaestel M, Engel K, Buchner J. Small heat shock proteins are molecular chaperones. J Biol Chem 1993;268:1517–20. [PubMed: 8093612]
2. Ciocca DR, Oesterreich S, Chamness GC, McGuire WL, Fuqua SA. Biological and clinical implications of heat shock protein 27,000 (Hsp27): a review. J Natl Cancer Inst 1993;85:1558–70. [PubMed: 8411230]
3. Ciocca DR, Calderwood SK. Heat shock proteins in cancer: diagnostic, prognostic, predictive, and treatment implications. Cell Stress Chaperones 2005;10:86–103. [PubMed: 16038406]
4. Evgrafov OV, Mersiyanova I, Irobi J, Van Den Bosch L, Dierick I, Leung CL, Schagina O, Verpoorten N, Van Impe K, Fedotov V, Dadali E, Auer-Grumbach M, Windpassinger C, Wagner K, Mitrovic Z, Hilton-Jones D, Talbot K, Martin JJ, Vasserman N, Tverskaya S, Polyakov A, Liem RK, Gettemans J, Robberecht W, De Jonghe P, Timmerman V. Mutant small heat-shock protein 27 causes axonal Charcot-Marie-Tooth disease and distal hereditary motor neuropathy. Nat Genet 2004;36:602–6. [PubMed: 15122254]
5. Merck KB, Groenen PJ, Voorter CE, de Haard-Hoekman WA, Horwitz J, Bloemendal H, de Jong WW. Structural and functional similarities of bovine alpha-crystallin and mouse small heat-shock protein. A family of chaperones. J Biol Chem 1993;268:1046–52. [PubMed: 8093449]
6. Rogalla T, Ehrnsperger M, Preville X, Kotlyarov A, Lutsch G, Ducasse C, Paul C, Wieske M, Arrigo AP, Buchner J, Gaestel M. Regulation of Hsp27 oligomerization, chaperone function, and protective activity against oxidative stress/tumor necrosis factor alpha by phosphorylation. J Biol Chem 1999;274:18947–56. [PubMed: 10383393]
7. Lavoie JN, Lambert H, Hickey E, Weber LA, Landry J. Modulation of cellular thermoresistance and actin filament stability accompanies phosphorylation-induced changes in the oligomeric structure of heat shock protein 27. Mol Cell Biol 1995;15:505–16. [PubMed: 7799959]
8. Lavoie JN, Hickey E, Weber LA, Landry J. Modulation of actin microfilament dynamics and fluid phase pinocytosis by phosphorylation of heat shock protein 27. J Biol Chem 1993;268:24210–4. [PubMed: 8226968]
9. Bryantsev AL, Loktionova SA, Ilyinskaya OP, Tararak EM, Kampinga HH, Kabakov AE. Distribution, phosphorylation, and activities of Hsp25 in heat-stressed H9c2 myoblasts: a functional link to cytoprotection. Cell Stress Chaperones 2002;7:146–55. [PubMed: 12380682]
10. Benndorf R, Hayess K, Ryazantsev S, Wieske M, Behlke J, Lutsch G. Phosphorylation and supramolecular organization of murine small heat shock protein HSP25 abolish its actin polymerization-inhibiting activity. J Biol Chem 1994;269:20780–4. [PubMed: 8051180]
11. Pandey P, Farber R, Nakazawa A, Kumar S, Bharti A, Nalin C, Weichselbaum R, Kufe D, Kharbanda S. Hsp27 functions as a negative regulator of cytochrome c-dependent activation of procaspase-3. Oncogene 2000;19:1975–81. [PubMed: 10803458]
12. Paul C, Manero F, Gonin S, Kretz-Remy C, Virot S, Arrigo AP. Hsp27 as a negative regulator of cytochrome C release. Mol Cell Biol 2002;22:816–34. [PubMed: 11784858]

13. Rane MJ, Pan Y, Singh S, Powell DW, Wu R, Cummins T, Chen Q, McLeish KR, Klein JB. Heat shock protein 27 controls apoptosis by regulating Akt activation. J Biol Chem 2003;278:27828–35. [PubMed: 12740362]

14. Arrigo AP. Hsp27: novel regulator of intracellular redox state. IUBMB Life 2001;52:303–7. [PubMed: 11895079]

15. Kampinga HH, Brunsting JF, Stege GJ, Konings AW, Landry J. Cells overexpressing Hsp27 show accelerated recovery from heat-induced nuclear protein aggregation. Biochem Biophys Res Commun 1994;204:1170–7. [PubMed: 7980592]

16. Doerwald L, van Genesen ST, Onnekink C, Marin-Vinader L, de Lange F, de Jong WW, Lubsen NH. The effect of alphaB-crystallin and Hsp27 on the availability of translation initiation factors in heat-shocked cells. Cell Mol Life Sci 2006;63:735–43. [PubMed: 16505970]

17. Marin-Vinader L, Shin C, Onnekink C, Manley JL, Lubsen NH. Hsp27 enhances recovery of splicing as well as rephosphorylation of SRp38 after heat shock. Mol Biol Cell 2006;17:886–94. [PubMed: 16339078]

18. Voorter CE, Wintjes L, Bloemendal H, de Jong WW. Relocalization of alpha B-crystallin by heat shock in ovarian carcinoma cells. FEBS Lett 1992;309:111–4. [PubMed: 1505673]

19. McClaren M, Isseroff RR. Dynamic changes in intracellular localization and isoforms of the 27-kD stress protein in human keratinocytes. J Invest Dermatol 1994;102:375–81. [PubMed: 8120422]

20. Loktionova SA, Ilyinskaya OP, Gabai VL, Kabakov AE. Distinct effects of heat shock and ATP depletion on distribution and isoform patterns of human Hsp27 in endothelial cells. FEBS Lett 1996;392:100–4. [PubMed: 8772183]

21. Adhikari AS, Sridhar Rao K, Rangaraj N, Parnaik VK, Mohan Rao C. Heat stress-induced localization of small heat shock proteins in mouse myoblasts: intranuclear lamin A/C speckles as target for alphaB-crystallin and Hsp25. Exp Cell Res 2004;299:393–403. [PubMed: 15350538]

22. Cotto J, Fox S, Morimoto R. HSF1 granules: a novel stress-induced nuclear compartment of human cells. J Cell Sci 1997;110 (Pt 23):2925–34. [PubMed: 9359875]

23. van den Ijssel P, Wheelock R, Prescott A, Russell P, Quinlan RA. Nuclear speckle localisation of the small heat shock protein alpha B-crystallin and its inhibition by the R120G cardiomyopathy-linked mutation. Exp Cell Res 2003;287:249–61. [PubMed: 12837281]

24. den Engelsman J, Bennink EJ, Doerwald L, Onnekink C, Wunderink L, Andley UP, Kato K, de Jong WW, Boelens WC. Mimicking phosphorylation of the small heat-shock protein alphaB-crystallin recruits the F-box protein FBX4 to nuclear SC35 speckles. Eur J Biochem 2004;271:4195–203. [PubMed: 15511225]

25. den Engelsman J, Gerrits D, de Jong WW, Robbins J, Kato K, Boelens WC. Nuclear import of alpha B-crystallin is phosphorylation-dependent and hampered by hyperphosphorylation of the myopathy-related mutant R120G. J Biol Chem 2005;280:37139–48. [PubMed: 16129694]

26. Geum D, Son GH, Kim K. Phosphorylation-dependent cellular localization and thermoprotective role of heat shock protein 25 in hippocampal progenitor cells. J Biol Chem 2002;277:19913–21. [PubMed: 11912188]

27. Wong JW, Shi B, Farboud B, McClaren M, Shibamoto T, Cross CE, Isseroff RR. Ultraviolet B-mediated phosphorylation of the small heat shock protein HSP27 in human keratinocytes. J Invest Dermatol 2000;115:427–34. [PubMed: 10951279]

28. Nollen EA, Kabakov AE, Brunsting JF, Kanon B, Hohfeld J, Kampinga HH. Modulation of in vivo HSP70 chaperone activity by Hip and Bag-1. J Biol Chem 2001;276:4677–82. [PubMed: 11076956]

29. Fey EG, Krochmalnic G, Penman S. The nonchromatin substructures of the nucleus: the ribonucleoprotein (RNP)-containing and RNP-depleted matrices analyzed by sequential fractionation and resinless section electron microscopy. J Cell Biol 1986;102:1654–65. [PubMed: 3700470]

30. He DC, Nickerson JA, Penman S. Core filaments of the nuclear matrix. J Cell Biol 1990;110:569–80. [PubMed: 2307700]

31. Shelden EA, Borrelli MJ, Pollock FM, Bonham R. Heat shock protein 27 associates with basolateral cell boundaries in heat-shocked and ATP-depleted epithelial cells. J Am Soc Nephrol 2002;13:332–41. [PubMed: 11805160]

32. Landry J, Chretien P, Lambert H, Hickey E, Weber LA. Heat shock resistance conferred by expression of the human HSP27 gene in rodent cells. J Cell Biol 1989;109:7–15. [PubMed: 2745558]
33. van de Klundert FA, Gijsen ML, van den IPR, Snoeckx LH, de Jong WW. alpha B-crystallin and hsp25 in neonatal cardiac cells--differences in cellular localization under stress conditions. Eur J Cell Biol 1998;75:38–45. [PubMed: 9523153]
34. Spector DL, Fu XD, Maniatis T. Associations between distinct pre-mRNA splicing components and the cell nucleus. Embo J 1991;10:3467–81. [PubMed: 1833187]
35. Heidenreich O, Neininger A, Schratt G, Zinck R, Cahill MA, Engel K, Kotlyarov A, Kraft R, Kostka S, Gaestel M, Nordheim A. MAPKAP kinase 2 phosphorylates serum response factor in vitro and in vivo. J Biol Chem 1999;274:14434–43. [PubMed: 10318869]
36. Lambert H, Charette SJ, Bernier AF, Guimond A, Landry J. HSP27 multimerization mediated by phosphorylation-sensitive intermolecular interactions at the amino terminus. J Biol Chem 1999;274:9378–85. [PubMed: 10092617]
37. Lamond AI, Spector DL. Nuclear speckles: a model for nuclear organelles. Nat Rev Mol Cell Biol 2003;4:605–12. [PubMed: 12923522]
38. Marin R, Tanguay RM. Stage-specific localization of the small heat shock protein Hsp27 during oogenesis in Drosophila melanogaster. Chromosoma 1996;105:142–9. [PubMed: 8781182]
39. Sun Y, Mansour M, Crack JA, Gass GL, MacRae TH. Oligomerization, chaperone activity, and nuclear localization of p26, a small heat shock protein from Artemia franciscana. J Biol Chem 2004;279:39999–40006. [PubMed: 15258152]
40. Butt E, Immler D, Meyer HE, Kotlyarov A, Laass K, Gaestel M. Heat shock protein 27 is a substrate of cGMP-dependent protein kinase in intact human platelets: phosphorylation-induced actin polymerization caused by HSP27 mutants. J Biol Chem 2001;276:7108–13. [PubMed: 11383510]
41. Eaton P, Fuller W, Shattock MJ. S-thiolation of HSP27 regulates its multimeric aggregate size independently of phosphorylation. J Biol Chem 2002;277:21189–96. [PubMed: 11925435]Epub 2002 Mar 29
42. Perez-Terzic C, Gacy AM, Bortolon R, Dzeja PP, Puceat M, Jaconi M, Prendergast FG, Terzic A. Structural plasticity of the cardiac nuclear pore complex in response to regulators of nuclear import. Circ Res 1999;84:1292–301. [PubMed: 10364567]
43. Borrelli MJ, Bernock LJ, Landry J, Spitz DR, Weber LA, Hickey E, Freeman ML, Corry PM. Stress protection by a fluorescent Hsp27 chimera that is independent of nuclear translocation or multimeric dissociation. Cell Stress Chaperones 2002;7:281–96. [PubMed: 12482204]
44. Aoyama A, Frohli E, Schafer R, Klemenz R. Alpha B-crystallin expression in mouse NIH 3T3 fibroblasts: glucocorticoid responsiveness and involvement in thermal protection. Mol Cell Biol 1993;13:1824–35. [PubMed: 8441415]
45. Mehlen P, Hickey E, Weber LA, Arrigo AP. Large unphosphorylated aggregates as the active form of hsp27 which controls intracellular reactive oxygen species and glutathione levels and generates a protection against TNFalpha in NIH-3T3-ras cells. Biochem Biophys Res Commun 1997;241:187–92. [PubMed: 9405255]
46. Knauf U, Jakob U, Engel K, Buchner J, Gaestel M. Stress- and mitogen-induced phosphorylation of the small heat shock protein Hsp25 by MAPKAP kinase 2 is not essential for chaperone properties and cellular thermoresistance. Embo J 1994;13:54–60. [PubMed: 7905823]
47. Panasenko OO, Kim MV, Marston SB, Gusev NB. Interaction of the small heat shock protein with molecular mass 25 kDa (hsp25) with actin. Eur J Biochem 2003;270:892–901. [PubMed: 12603322]
48. Bond U. Heat shock but not other stress inducers leads to the disruption of a subset of snRNPs and inhibition of in vitro splicing in HeLa cells. Embo J 1988;7:3509–18. [PubMed: 2974799]
49. Shin C, Kleiman FE, Manley JL. Multiple properties of the splicing repressor SRp38 distinguish it from typical SR proteins. Mol Cell Biol 2005;25:8334–43. [PubMed: 16135820]
50. Prasanth KV, Prasanth SG, Xuan Z, Hearn S, Freier SM, Bennett CF, Zhang MQ, Spector DL. Regulating gene expression through RNA nuclear retention. Cell 2005;123:249–63. [PubMed: 16239143]
51. Mounier N, Arrigo A. Actin cytoskeleton and small heat shock proteins: how do they interact? Cell Stress Chaperone 2002;7:167–176.

52. Quinlan R. Cytoskeletal competence requires protein chaperones. Prog Mol Subcell Biol 2002;28:219–33. [PubMed: 11908062]

53. van Rijk AE, Stege GJ, Bennink EJ, May A, Bloemendal H. Nuclear staining for the small heat shock protein alphaB-crystallin colocalizes with splicing factor SC35. Eur J Cell Biol 2003;82:361–8. [PubMed: 12924631]

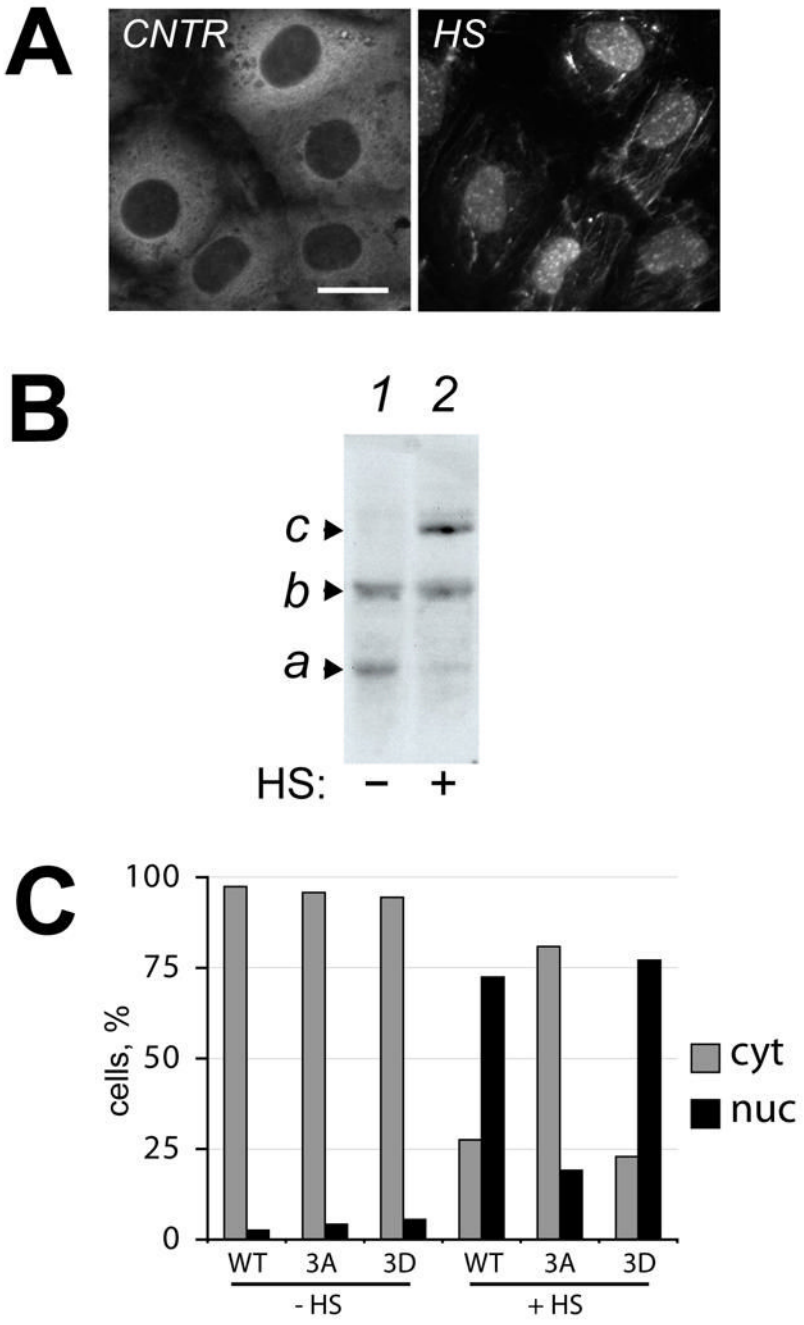

Figure 1. Phosphorylation of Hsp27 accompanies its translocation to the nucleus of NRK renal epithelial cells during heat shock

A. Rat Hsp25 is detected in the cytosol of control NRK cells but associates with the nucleus and cytoskeleton after heat shock (43 °C for 30 minutes). Bar, 20 μm. **B.** IEF analysis of rat Hsp25 phosphorylation shows an increased presence of phosphorylated Hsp27 isoforms (*b*, *c*) and a decrease in non-phosphorylated Hsp27 (*a*) in lysates of heat shocked cells (lane 2) compared to non-stressed control (lane 1). **C.** Quantitative analysis of the fraction of cells with exogenously expressed human Hsp27 in nuclei after incubation under control conditions (−HS) or after heat shock for 30 minutes at 43°C (+HS). All exogenously expressed proteins were predominately found in the cytoplasm (grey bars) under control conditions. Heat shock induced

translocation to the nucleus (black bars) of exogenous wild-type Hsp27 (WT) and phosphorylation-state mimicking Hsp27 (3D) but not a non-phosphorylatable Hsp27 mutant (3A).

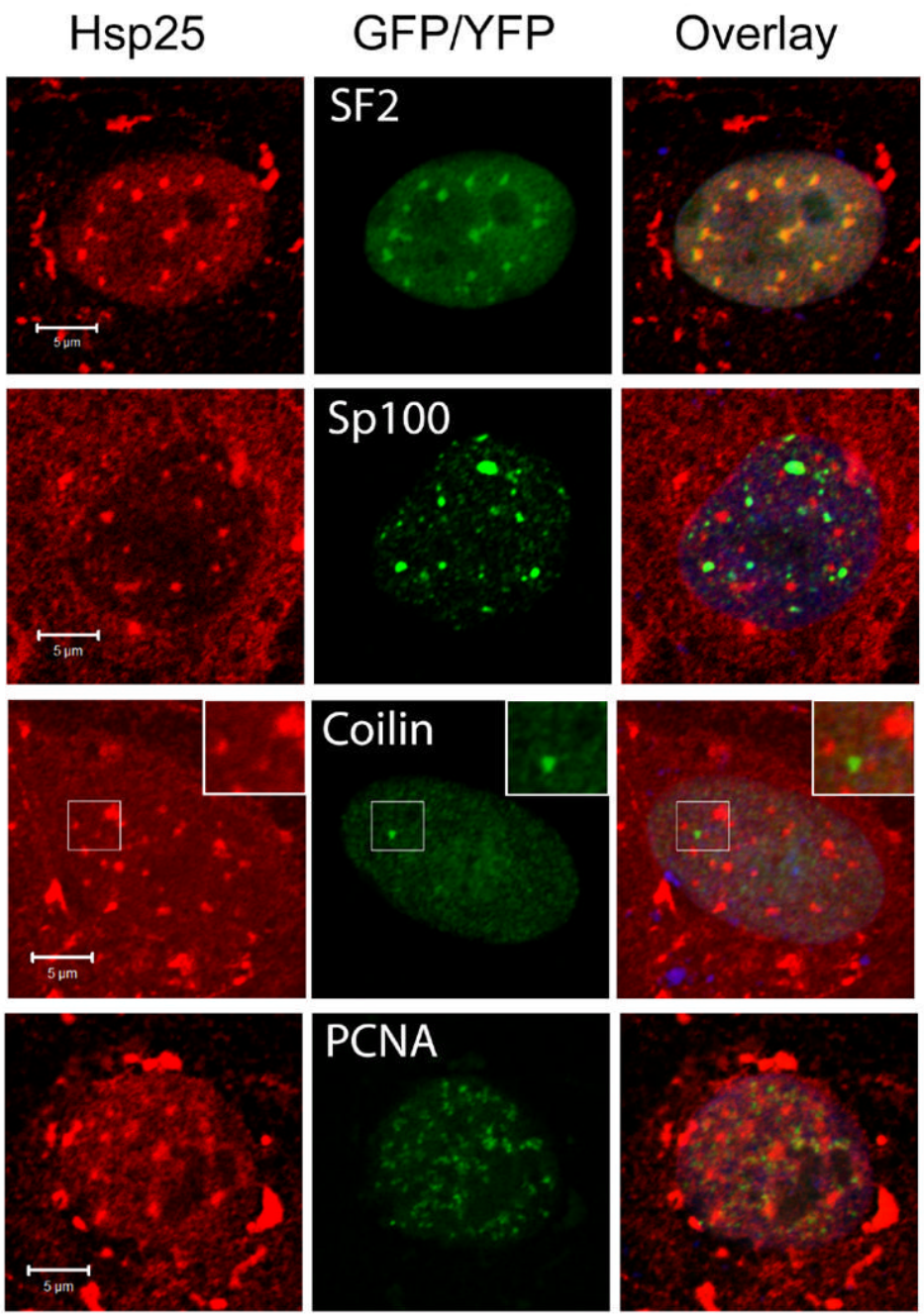

Figure 2. Hsp27 specifically associates with nuclear speckles in heat shocked NRK cells

NRK cells transfected with plasmids coding for SF2-EGFP, Sp100-YFP, coilin-EGFP, or PCNA-EGFP, were heat shocked at 43°C for 60 minutes and processed to detect fusion proteins (green), Hsp25 (red) and DNA (blue) by confocal microscopy. Color overlay images show that Hsp25 co-localizes with a marker for nuclear speckles (SF2), but not with markers for PML bodies (Sp100), active replication sites (PCNA) or Cajal bodies (coilin). Coilin containing Cajal bodies were sometimes found in close proximity to Hsp25 positive nuclear speckles (inset, merged image and selected region in Hsp25 and coilin-EGFP images). Bars, 5 μm.

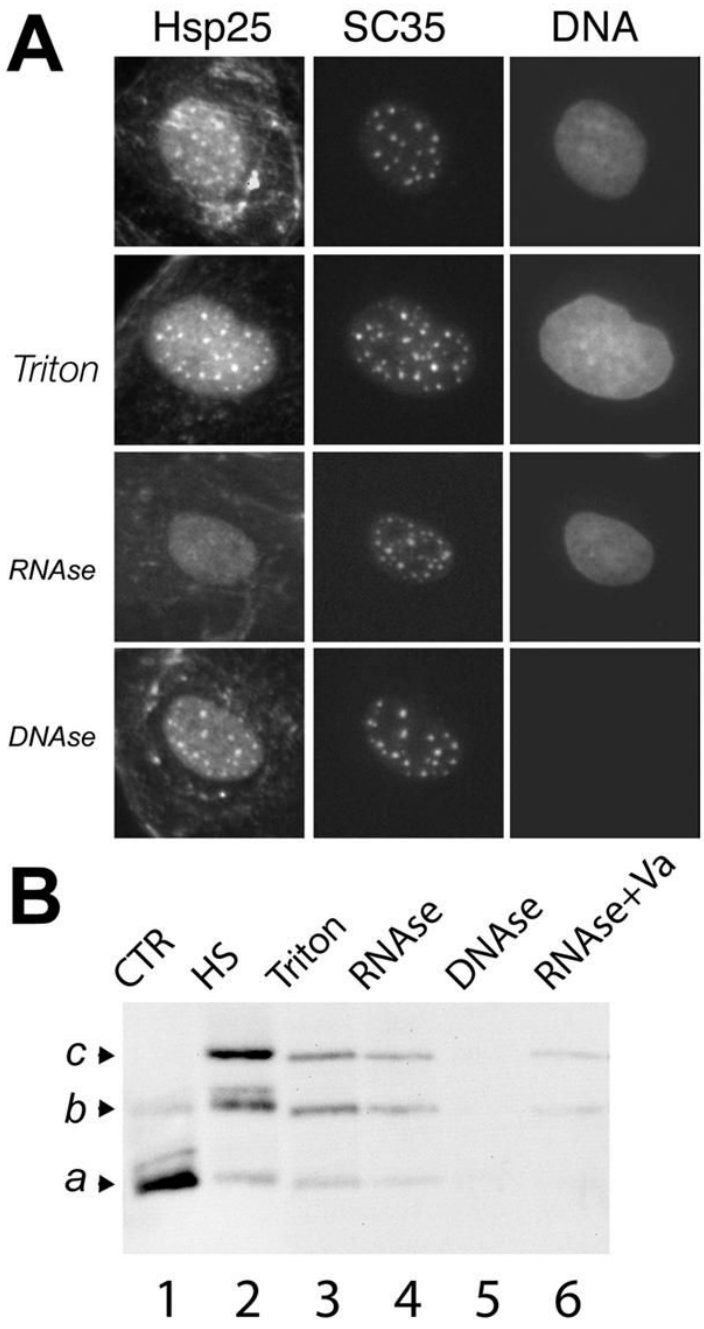

Figure 3. Phosphorylated Hsp27 associates with an RNAse soluble fraction of nuclear speckles

A. Heat shocked NRK cells were processed for fluorescence localization of Hsp27, SC35 and DNA. Hsp27 associates with SC35 containing nuclear speckles in intact cells (top panels), after detergent lysis (*Triton*) and after detergent lysis followed by DNAse digestion (*DNAse*, note loss of DNA staining), but not after digestions with buffers containing RNAse (*RNAse*). Bar, 20 μm. **B.** IEF gel electrophoresis and Hsp25 immunoblotting of whole cell lysates isolated under control conditions (CNTR) or after heat shock (HS) and of protein fractions released by various extraction procedures. Hsp25 released by RNAse digestion of detergent lysed cells (RNAse) is predominately mono- (*b*) and bi-phosphorylated (*c*). Relatively little Hsp25 is

released from detergent lysed cells using DNAse (DNAse) or RNAse in the presence of the RNAse inhibitor (RNAse+Va).

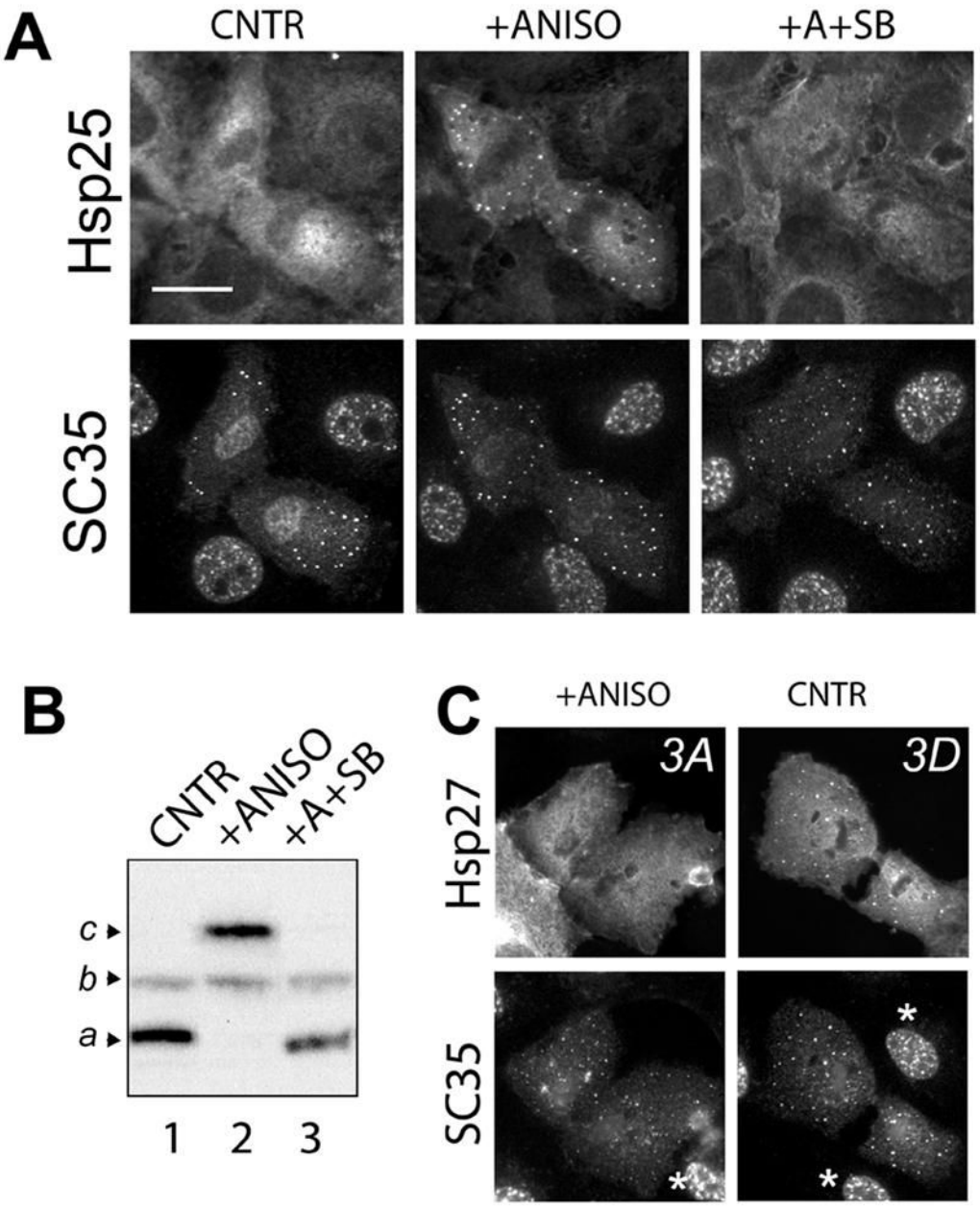

Figure 4. Phosphorylated Hsp27 associates with mitotic interchromatin granules without stress

A. Late anaphase and telophase NRK cells processed for detection of endogenous Hsp27 and SC35 are shown under control conditions (CNTR), after treatment with anisomycin, a p38 MAPK activator (+ANISO), and after combined treatment with anisomycin and SB202190, a specific p38 MAPK inhibitor (+ANISO+SB). Co-localization of endogenous Hsp27 and SC35 positive nuclear speckles is detected in cells treated with anisomycin alone (+ANISO), but not other conditions. **B.** Anisomycin treatment results in an enhanced phosphorylation (*b, c*) of Hsp27 (+ANISO), which is inhibited by co-treatment with SB202190 (+A+SB). **C.** Transiently expressed human mutant Hsp27 lacking phosphorylatable serines (3A) fails to associate with SC35 positive speckles in telophase cells even after anisomycin treatment (+ANISO), while the phosphorylation-state mimicking Hsp27 mutant (3D) associates with these nuclear

speckles, even in untreated cells (CNTR). Asterisks (*) indicate cells lacking detectable expression of exogenous Hsp27 proteins. Bars, 20 μm.

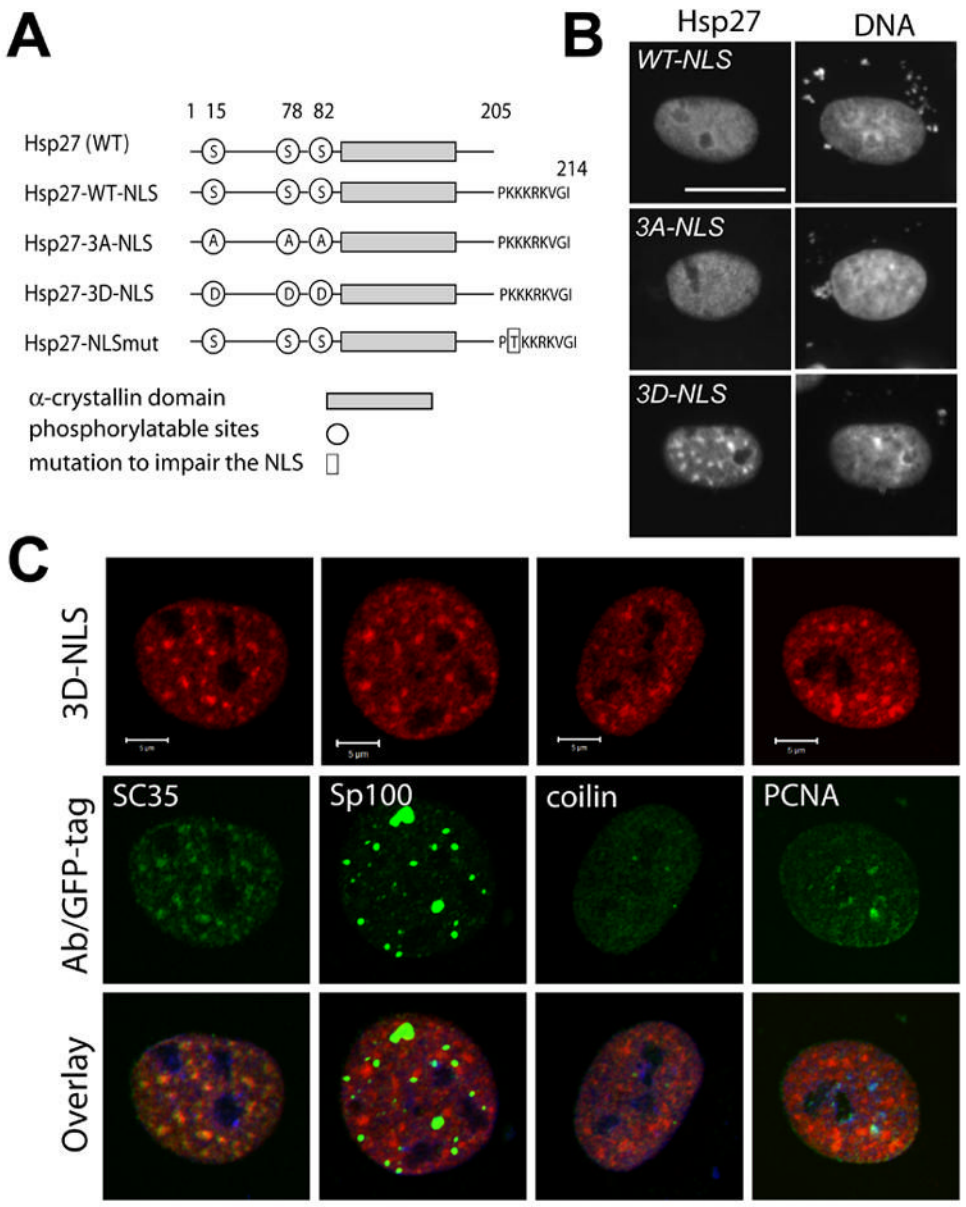

Figure 5. NLS-tagged Hsp27 differentially associates with nuclear substructure

A. Organization of wild type Hsp27 and various NLS-tagged mutants. **B.** Localization of NLS-tagged proteins Hsp27-WT-NLS (*WT-NLS*), Hsp27-3A-NLS (*3A-NLS*), and Hsp27-3D-NLS (*3D-NLS*) in transiently transfected NRK cells (Hsp27) and counterstained for DNA (DNA). The mutant protein mimicking constitutive phosphorylation (*3D-NLS*), but not other proteins, forms a speckled pattern within the nucleus. Bar, 20 μm. **C.** Confocal analysis of double labeled, transiently transfected cells, cultured under control conditions, shows co-localization of an NLS-tagged phosphorylation mimicking Hsp27 mutant (3D-NLS) with a marker for nuclear speckles (SC35) in the absence of stress (yellow/orange, Overlay), but not with markers for PML bodies (Sp100), Cajal bodies (coilin) or active replication sites (PCNA). Bars, 5 μm.

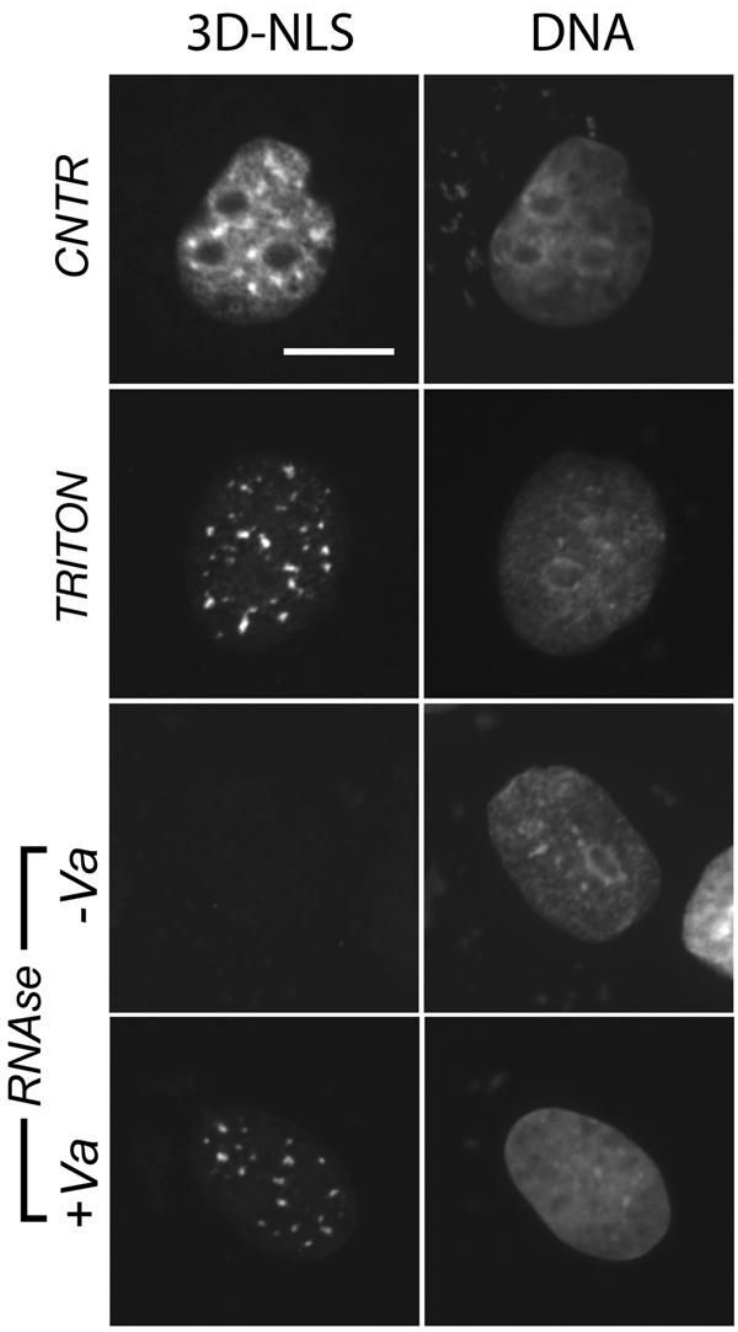

Figure 6. The NLS-tagged human Hsp27 mutant mimicking constitutive phosphorylation localizes to an RNAse soluble fraction of nuclear speckles in unstressed cells

Distribution of Hsp27-3D-NLS under control conditions and after extractions. Nuclear speckle-associated Hsp27-3D-NLS (*CNTR*) is insoluble after detergent lysis (*Triton*), but is extracted from lysed cells using RNAse (−Va). RNAse inhibitor prevents the extraction of Hsp27 (+Va). Bar, 10 μm.

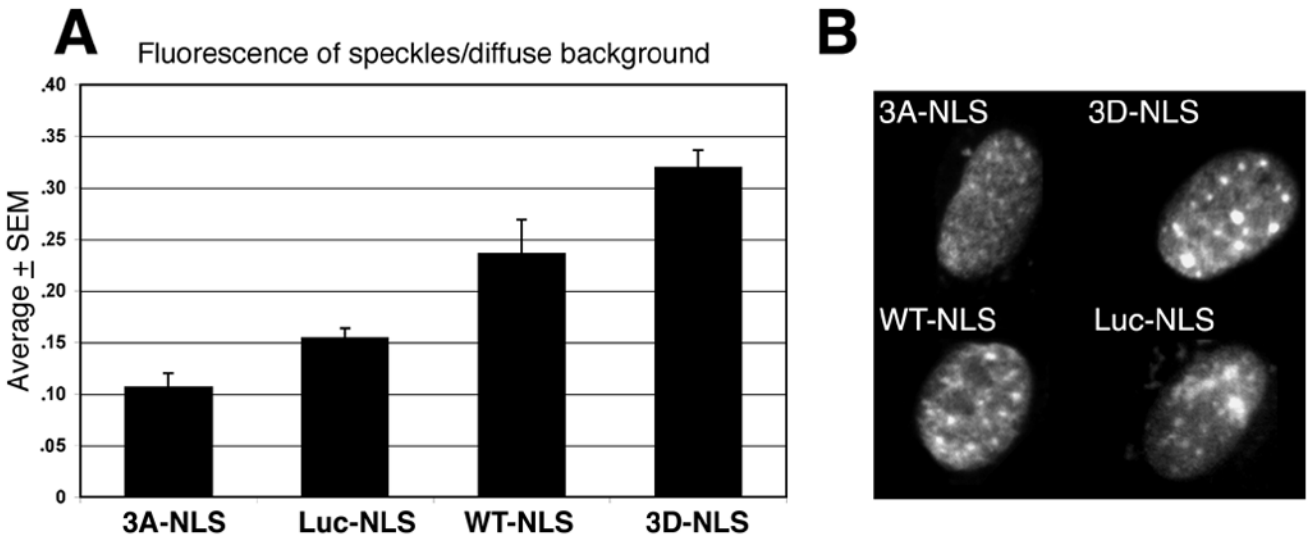

Figure 7. Association of NLS-tagged proteins with nuclear speckles in heat shocked NRK cells

A. The ratio of nuclear fluorescence found associated with speckles and nuclear fluorescence not associated with speckles measured in individual cells. The average + SEM values are 10.7 +1.3 (NLS-3A), 15.5+.9 (NLS-Luc), 23.7+3.2 (NLS-WT) and 32.0+1.6 (NLS-3D). Values were calculated from 366 speckles in 37 cells (NLS-3A), 168 speckles in 13 cells (NLS-Luc), 640 speckles in 41 cells (NLS-Wt) and in 501 speckles in 28 cells (NLS-3D). All mean values were statistically compared to all others using a Student's *T* test and were statistically different ($p<.05$). **B.** Representative images of NLS-tagged protein distribution and fluorescence intensity in heat shocked NRK cells. These cells were selected for display because their computed ratio of fluorescence found in speckles/non-speckle background was the median value for the pool of cells analyzed in each test group.

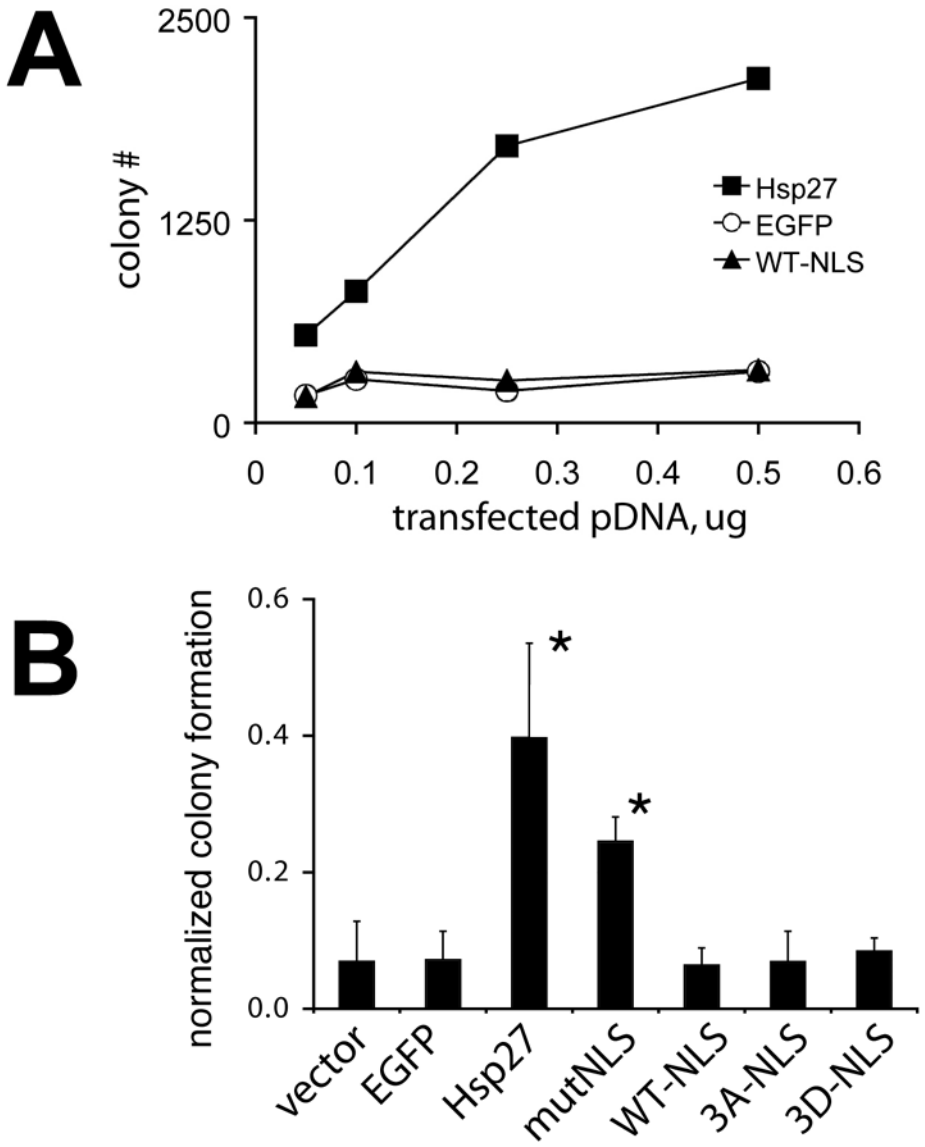

Figure 8. Targeting of human Hsp27 to the nucleus does not alter cellular thermotolerance

A. Colony formation of NIH3T3 cells heat shocked (44°C for 3.5 hours) after transfections with increasing amounts of plasmid coding for green fluorescent protein (EGFP, open circles), human Hsp27 wild type (Hsp27, closed squares), and Hsp27-WT-NLS (WT-NLS, closed triangles). **B.** Colony formation of NIH3T3 cells heat shocked (44°C for 3.5 hours) after transfection with 0.5 μg of the indicated plasmid DNA. Nuclear Hsp27 proteins do not enhance or diminish colony formation after heat shock, relative to cells transfected with empty vector (vector) or an unrelated protein (EGFP). However, Hsp27 tagged with a nonfunctional NLS (mutNLS) does enhance thermotolerance. The averages and standard deviations obtained from analysis of three independent experiments are shown. Asterisks denote experiment producing numbers of colonies significantly greater than empty vector control transfections ($p<.05$).

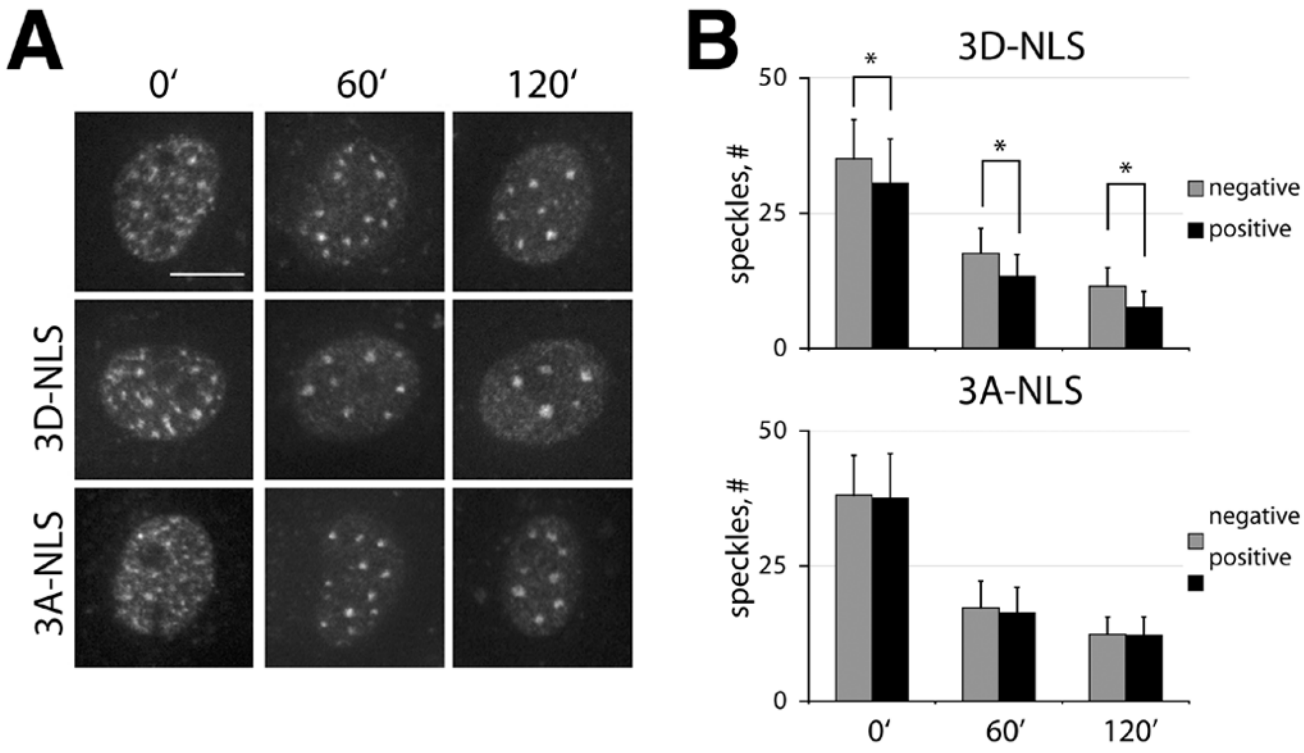

Figure 9. SC35-positive nuclear speckles are altered by Hsp27-3D-NLS

A. NRK cells expressing the indicated proteins (3D-NLS, 3A-NLS) and nontransfected cells (unlabeled top panels) were treated with 2 μg/ml actinomycin D for 0′, 60′, and 120′, then fixed and immunostained to detect human Hsp27 (not shown) and SC35 positive nuclear speckles. Representative staining for SC35 is shown. **B.** Quantitative analysis of the number of nuclear speckles in cells expressing the indicated NLS tagged Hsp27 mutant (positive, black bars) and non-expressing neighbors (negative, grey bars). Expression of Hsp27-3D-NLS, but not Hsp27-3A-NLS alters the number of nuclear speckles in all groups, relative to non-expressing controls. Asterisks indicate those average values significantly different from that of internal negative controls ($p \leq .05$).

Table 1

Number, measured area, fluorescence intensity (FI) and calculated volume of anti-SC35 immunostained nuclear speckles in NRK cells expressing the Hsp27-3D-NLS mutant protein and neighboring non-expressing control cells after 120 minutes treatment with actinomycin D

Values shown are the average ± standard errors obtained from 288 nuclear speckles in 43 Hsp27-3D-NLS expressing cells and 413 nuclear speckles in 41 non-expressing cells. Ratios were calculated by dividing mean values obtained from Hsp27-3D-NLS expressing cells divided by mean values obtained from non-expressing controls. Cells expressing Hsp27-3D-NLS had greater average values for area, fluorescence intensity and calculated volume than non-expressing neighbors but fewer nuclear speckles. Asterisks identify those parameters where values obtained from control non-expressing cells are significantly different ($p \leq 0.01$) than corresponding values obtained from Hsp27-3D-NLS expressing cells.

	Control	Hsp27-3D-NLS	Ratio of means
Number per nucleus*	11.5±3.4	7.6±2.9	0.66
Area (pixels^2)*	65.4±1.9	77.8±2.8	1.19
FI *	12398±402	16685±690	1.35
Volume (pixels^3)*	443.5±21.9	584.8±34.5	1.32